

LETTER

Open Access



Uniform formation and characterization of Au/TiO₂ nanoparticles for electrokinetically assisted optofluidic reactors

Eunseok Seo¹, Jaehyun Jung¹, Cong Wang² and Jungyul Park^{1*}

Abstract

Research is being conducted on photocatalyst-based organic compound treatment processes for water purification to decompose wastewater efficiently. An optofluidic reactor based on TiO₂ photocatalysis and nanoelectrokinetics was presented recently to improve the efficacy of photocatalytic water purification. However, inefficient absorption of visible light by TiO₂ materials hinders the effective utilization of solar energy. To address this issue, the uniform formation and characterization of Au/TiO₂ nanoparticles for a plasmonic photocatalytic-based optofluidic platform are studied to improve photocatalytic reactivity in visible light. The present study uses UV irradiation and spray spraying for producing Au/TiO₂ NPs uniformly on microporous carbon fabric. Energy dispersive X-ray analysis (EDX), X-ray photoelectron spectroscopy (XPS), transmission electron microscopy (TEM), scanning electron microscopy (SEM), and X-ray diffraction (XRD) were used to assess the quality of the Au/TiO₂ NP-coated carbon fabric. Au NPs were uniformly obtained on the surface and inside the TiO₂ coating layer by UV irradiation-based photo-reduction, according to SEM and TEM investigation. The interaction of Au NPs, TiO₂ NPs, and carbon fabric (CF) to improve electron transport and charge separation on the photocatalyst surface is supported by XPS spectra. TEM and XRD analyses revealed that all TiO₂ components in the Au/TiO₂ coating layer consisted of anatase having high photocatalytic activity. After comparing the photocatalytic activity of TiO₂ and Au/TiO₂-coated samples under solar-simulated light and a voltage of 3 V, it was found that the surface coated with Au NPs had a superior photocatalytic effect than the surface coated with only TiO₂.

Keywords Photocatalysis, Optofluidics, Water purification, Plasmonic, Electrokinetics, Nanoparticles

Introduction

Photocatalysis has received a lot of attention because it can not only convert CO₂ (the main cause of global warming) into useful hydrocarbons like methane and methanol [1, 2], but it can also produce oxygen and hydrogen through water-splitting reactions [3, 4] and

purify water by decomposing toxic organic pollutants [5, 6] and microplastics [7, 8]. Regarding photocatalytic performance, reactor designs play a crucial role in photocatalytic efficiency. Compared to the traditional photocatalytic reactors, photocatalytic optofluidic microreactors are a promising technique that brings together the advantages of microfluidics with photocatalysis, providing high surface-to-volume ratio, short molecular diffusion length, and high reaction efficiency [9]. Recently, research has been conducted to increase the efficiency of optofluidic-based wastewater treatment technology by enhancing photocatalysis using a nonlinear electric field in a microchannel [10]. UV light can induce the heterogeneous photocatalysis of titanium dioxide (TiO₂), which

*Correspondence:

Jungyul Park
sortpark@sogang.ac.kr

¹ Department of Mechanical Engineering, Sogang University, 35 Baekbeom-ro (Sinsu-dong), Mapo-gu, Seoul 04107, Republic of Korea

² School of Mechanical Engineering and Electronic Information, China University of Geosciences (Wuhan), 388 Lumo Road, Wuhan 430074, China

can then oxidize organic molecules adsorbing on the surface of the material into non-toxic compounds like CO_2 and H_2O [11, 12]. However, the ineffective absorption of visible light by pure TiO_2 materials restricts the effective use of solar energy [13, 14]. For photocatalytic water purification technology to be easily applied in an outdoor setting, photocatalytic reactions must be able to occur actively even by sunlight sources.

In this study, a plasmonic photocatalytic-based optofluidic platform is developed through the simple and uniform formation of Au/TiO_2 nanoparticles (NPs) on porous carbon fabric to overcome existing limitations. Au/TiO_2 NPs serve as plasmonic materials and enhance photocatalytic activity in visible light. Combining Au nanoparticles and TiO_2 is an effective strategy to enhance the spectral responsiveness of photocatalysts to the visible light spectrum. In addition, it can also leverage photothermal effects to accelerate the degradation process for organic compounds. The use of Au/TiO_2 NP photocatalysts in combination with porous carbon fabric can enhance catalyst reactivity, efficiency, and sustainability due to their high surface-to-volume ratio. This combination can also improve charge carrier separation and decrease charge transfer resistance between TiO_2 and carbon.

Materials and methods

Optofluidic reactor fabrication and Au/TiO_2 NPs synthesis

The components of the optofluidic microreactor include a PMMA plate, a carbon fabric (CF) coated with Au/TiO_2 NPs, a silicone rubber spacer with a microchannel pattern, and a Nafion-coated indium-tin-oxide (ITO)-coated glass (Omniscience, Korea) from bottom to top.

To improve the stability of the TiO_2 suspension, sodium hexametaphosphate (SHMP; 96%, Sigma-Aldrich, Korea) was added as an inorganic stabilizer. The carbon fabric was made of microporous layer (MPL) coated with 30% PTFE waterproofing on its underside (410- μm thick, W1S1011, NARA Cell-Tech, Korea). The MPL was employed to prevent significant water flooding in the carbon fabric and to provide adequate O_2 exchange. An ultrasonic bath (DAIHAN Scientific, Korea) was used to sonicate a 100 ml TiO_2 nanoparticle suspension comprising 25 mg/ml TiO_2 NPs (Aeroxide P25, Sigma-Aldrich, Korea) and 1 mg/ml SHMP for 10 min. 400 ml of isopropyl alcohol (IPA) was mixed with the suspension before being sprayed onto carbon fabric (10 cm x 10 cm). The samples were baked for 5 min at 220 °C after being dried at 80 °C. After washing with water, transfer the specimen to a 1mM gold (III) chloride trihydrate ($\text{HAuCl}_4 \cdot 3\text{H}_2\text{O}$, Sigma-Aldrich, Korea) solution and irradiate 500 W UV (365 nm UV LED, MERHOLE, China) for 4 h to form Au

NPs on TiO_2 . Then wash with ethanol and dry at room temperature.

A cutting device (Portrait 3, Silhouette Inc.) was used to define the microchannel pattern in the silicone rubber sheet. The width and length of the flow channel were fixed at 2 and 190 mm, respectively. The microchannel height was fixed at 200 μm by the thickness of the silicon spacer. A Nafion solution (600 μL , 5% w/w in water and 1-propanol, D-521, Alfa Aesar) was uniformly applied to the electrically conductive side of the ITO glass (6.5 x 3 cm) and baked at 80 °C for 1 h to remove the solvent and form a thin Nafion membrane with an average thickness of 10 μm . The TiO_2 -nanoparticle-coated carbon fabric, silicone rubber spacer with a microchannel pattern, and ITO glass with a Nafion coating were then adhered layer by layer and sealed with silicone adhesive (3140 RTV Coating, DOWSIL™). In order to make the optofluidic reactor easier to handle and connect with tubing, poly methyl methacrylate (PMMA) plates were laser-cut into the required pattern and assembled with the device.

Characterizations

TEM and SEM imaging

The particle morphologies of the TiO_2 and Au NPs of the CF/ Au/TiO_2 samples were examined using a high resolution-transmission electron microscope (HR-TEM, JEOL 2100 F, JEOL, Japan) at 200 kV. The elemental analyses of the Au/TiO_2 samples were conducted using an energy dispersive X-ray spectroscope (EDX) equipped in the HR-TEM.

The surface morphologies of the CF/ Au/TiO_2 samples were examined using a field-emission scanning electron microscope (FE-SEM, JSM-7100 F, JEOL, Japan). The elemental analyses of the CF/ Au/TiO_2 samples were conducted using an energy dispersive X-ray spectroscope (EDX) equipped in the FE-SEM after coating the samples with platinum.

XPS and XRD measurements

X-ray Photoelectron spectra (XPS, PHI 5000 VersaProbe, Ulvac-PHI, Japan) of CF/ Au/TiO_2 samples were measured with an XPS equipment of the advanced analysis center of Korea Institute of Science and Technology (KIST). The chemical states of the component element of CF/ Au/TiO_2 were analyzed by XPS. X-ray diffraction (XRD) measurements were conducted using an X-ray diffractometer (Dmax2500/PC, 2theta scan, GIXRD for thin-film XRD) of the advanced analysis center of KIST.

Photocatalytic degradation

Photocatalytic degradation of rhodamine 6G (R6G, Sigma-Aldrich, Korea) was carried out in the optofluidic

reactor using a solar simulator at room temperature. A 50 μM concentration of R6G solution was injected into the prepared optofluidic reactor using a syringe pump (NE-1000, New Era Pump Systems Inc., Farmingdale, NY, USA). The photocatalytic reaction was performed in a standard AM-1.5 solar simulated light of the same wavelength and intensity (1 sun=1000 W/m²) using a solar simulator (PEC-L01, Peccell Technologies, Japan). A microplate reader (BKMPR-1011, Konvision Inc. Korea) was used to measure the absorption spectra after the degraded R6G solution was collected from the outlet. Using a picoammeter/voltage source (6487, Keithley Instrument), a potential bias was applied between the carbon fabric and ITO glass. Using the LabVIEW program, a computer linked to the picoammeter/voltage source via a GPIB card (PCI-GPIB, National Instruments) captured the voltage and current signals.

The absorption spectra of the R6G solution that was collected from optofluidic reactor were measured using a microplate reader. The degradation percentage of R6G (η_{deg}) was calculated using the following equation:

$$\eta_{deg} = \frac{I_0 - I}{I_0} \times 100\%$$

where I_0 and I are the absorbances of the R6G solution before and after the photocatalytic reaction, respectively. The degradation percentage was evaluated by monitoring the absorbance change of the R6G solution at a wavelength of 492 nm.

Results and discussion

TEM analyses of Au/TiO₂ NPs

The three processes that led to the successful fabrication of the CF/Au/TiO₂ composite were TiO₂ spray coating and thermal reaction, and photo-reduction of Au NPs by UV light (Fig. 1A).

The morphology and element analysis of TiO₂ or Au NPs were studied by HR-TEM and EDX analyses, respectively. An enlarged observation (Fig. 1C) of the TiO₂ coated parts of the TEM image (Fig. 1B) shows that the anatase particles are connected to each other and formed in cotton balls on the carbon fibers by thermal reaction when spray coating and drying are repeatedly carried out on a hot plate at 80 °C and then baked at 220 °C. Lattice fringes (d-spacing) of approximately 0.33 and 0.35 nm are observed in the matching HR-TEM image (Fig. 1C), which can be indexed as the (101) plane of anatase TiO₂. The ternary composite “CF/Au/TiO₂” is created by loading Au NPs using the photo-reduction technique by UV light after the CF/TiO₂ has been prepared. Figure 1D and E show EDX elemental mapping image and the EDX analyses of the CF/Au/TiO₂, respectively. As shown in Fig. 1D, Au NPs are evenly distributed on the surface and inside of the TiO₂ cotton balls.

SEM analyses of Au/TiO₂ NPs

The components of the optofluidic microreactor include a PMMA plate, a CF/Au/TiO₂ composite, a silicone rubber spacer with a microchannel pattern, and a Nafion-coated indium-tin-oxide (ITO)-coated glass from bottom

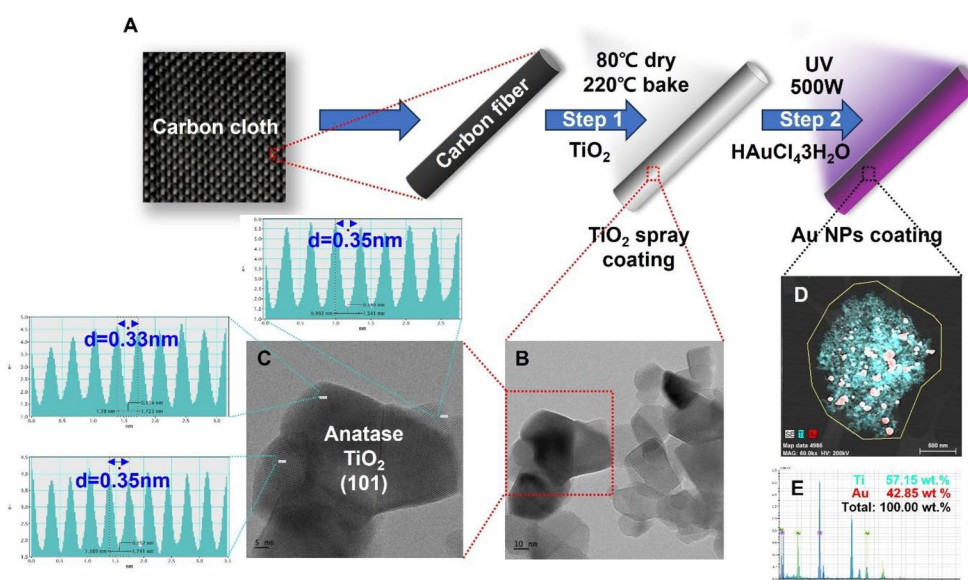


Fig. 1 A Diagrammatic representation of the experimental techniques used for coating the Au/TiO₂ on carbon fabric. B, C TEM images of TiO₂ in low- and high-resolution (HR). D, E TEM image and EDX elemental (Ti, Au) mappings of the Au/TiO₂ NPs on carbon fabric (CF)

to top (Fig. 2A, B). The surface of the TiO_2 photocatalyst coating needs to be coated with Au NPs to have a photocatalytic reaction using visible light energy. In this study, the morphology and element analysis of CF/Au/ TiO_2 after coating and synthesis of TiO_2 and Au NPs were studied by SEM and EDX analyses, respectively. Figure 2C shows a schematically illustration about the CF/Au/ TiO_2 's photocatalytic reaction mechanism when exposed to visible light. As shown in Fig. 2D–G, the synthesized Au NPs on the TiO_2 coated carbon fabric are evenly dispersed on the surface in the form of single NPs. Figure 2H shows EDX patterns of an Au/ TiO_2 NPs coating samples. Additional confirmation of the interaction among Au NPs, TiO_2 NPs, and CF can be obtained using XPS and XRD analysis.

XPS analysis of Au/ TiO_2 NPs

In order to study the electrical structure, oxidation state, chemical composition and interaction among TiO_2 NPs, Au NPs and CF, XPS analysis was used. Figure 3A–D show the high resolution XPS spectra of the CF/Au/ TiO_2 to characterize the valance states and the chemical environment of atoms of main elements (C, O, Ti, and Au) on the prepared composite surface. The XPS spectrum

of C 1 s can be fitted to two peaks. The peak with the binding energy of 284.6 eV is attributed to C–C and C=C bond from CF (Fig. 3A). The peak with the binding energy of 291.8 eV is attributed to C–F₂ bond from CF and waterproof coating (Fig. 3A). The O 1 s spectrum displays a peak at 531.0, which are ascribed to lattice oxygen of TiO_2 (Fig. 3B). The peaks located at binding energies of 465.5 and 459.8 eV are designated to the Ti 2p_{3/2} and Ti 2p_{1/2} spin-orbital splitting photoelectrons in the Ti⁴⁺ oxidation state, respectively, slightly shifting toward higher binding energy, compared with those of the pure bulk anatase. This shifting can be attributed to the transfer of conduction band electron of TiO_2 to the CF and/or Au NPs. The spin-orbital splitting between Ti 2p_{3/2} and Ti 2p_{1/2} (5.7 eV) is accordance with the chemical state of Ti⁴⁺ in the anatase TiO_2 (Fig. 3C). The peaks of Au 4f_{7/2} and Au 4f_{5/2} are located at 84.3 and 88.0 eV respectively, with the splitting of 3.7 eV, indicating loading Au NPs on TiO_2 (Fig. 3D). Overall, the XPS spectra support the interaction among Au NPs, TiO_2 NPs, and CF, which could enhance electron transport and charge separation on the photocatalyst surface. Additional confirmation of this can be obtained using TEM, SEM, and XRD analysis [15].

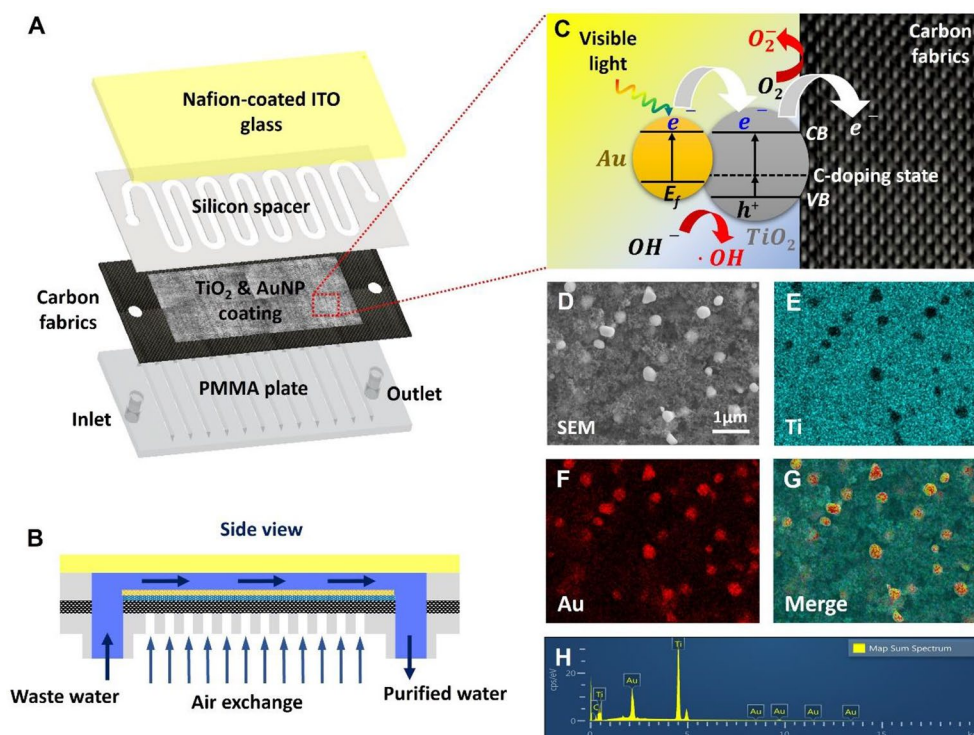


Fig. 2 **A** The optofluidic reactor consists of Nafion-coated ITO glass, silicon spacer, TiO_2 and Au nanoparticle-coated carbon fabrics (CFs), and PMMA plate. **B** Cross sectional view of the optofluidic reactor. **C** Principle of the CF/Au/ TiO_2 's photocatalytic reaction when exposed to visible light. **D** SEM images of the Au/ TiO_2 NPs coating sample. **E–G** EDX elemental mapping images of Ti and Au for the CF/Au/ TiO_2 . **H** EDX pattern of the Au/ TiO_2 NPs coating sample

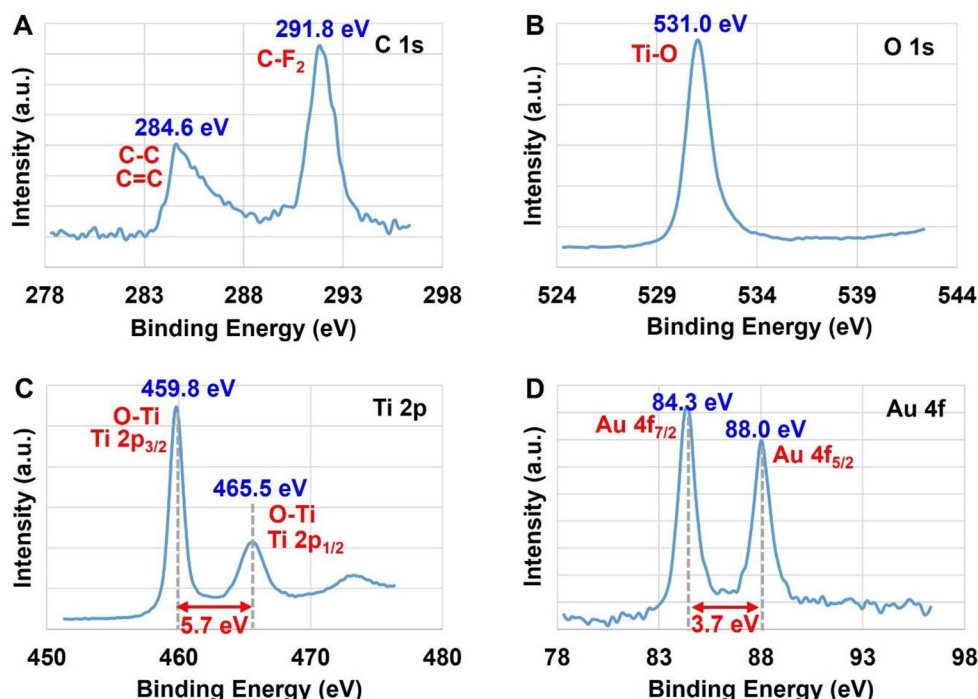


Fig. 3 High resolution XPS spectra of C 1s (A), O 1s (B), Ti 2p (C) and Au 4f (D) of the CF/Au/TiO₂

XRD analysis of Au/TiO₂ NPs

The crystal structure of Au/TiO₂ was investigated by XRD analysis (Fig. 4). XRD graph shows that rutile is absent and all of the TiO₂-coated surfaces produced in this experiment are anatase phase, which is expected to show high photocatalytic activity [16]. This is supported not only by the XRD pattern of the material, but also by the TiO₂ crystal structure shown in the HR-TEM image (Fig. 1C). This may be due to synthesis of TiO₂ or Au/TiO₂ was carried out at lower temperature. Another possibility may be that rutile particles that are not connected

to the anatase were removed during the washing process. The XRD data of the prepared a CF/Au/TiO₂ are used to identify the crystallographic phases of the product, along with three groups of data including TiO₂, Au NPs and CF. The peak at 2θ = 17° is identified as a typical carbon peak for CF. The obtained CF/Au/TiO₂'s XRD spectrum demonstrates that the dominant crystallographic phase of the TiO₂ generated in the CF/Au/TiO₂ composite is anatase TiO₂. TiO₂ in anatase crystal form has a high electron mobility, low mass density, and low dielectric constant. Furthermore, the featured peaks are indexed to the metal

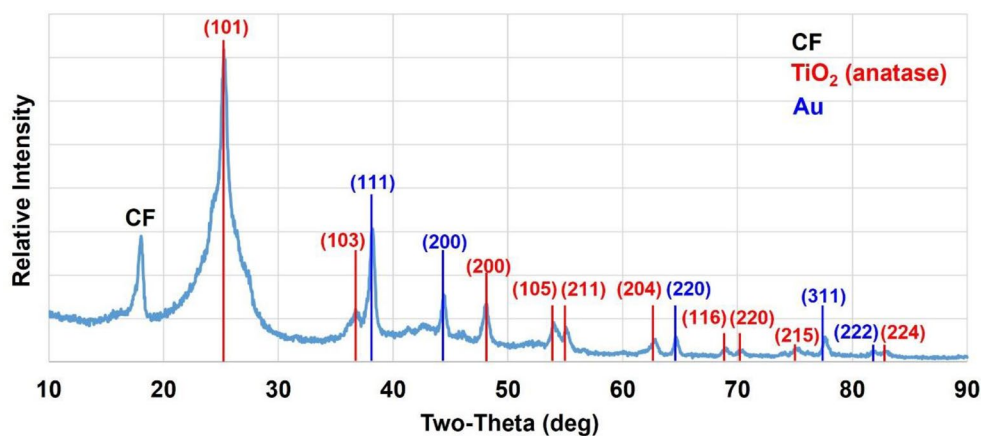


Fig. 4 XRD pattern of the CF/Au/TiO₂

Au phase's (111), (200), (220), (311) and (222) crystal planes, indicating that metallic Au is formed in the CF/Au/TiO₂ composite. The effective synthesis of a number of composites containing Au and anatase TiO₂ crystals shows that the composites have strong photocatalytic activity when exposed to visible light.

Comparison of photocatalytic degradation efficiency

In preliminary test, we observed the degradation efficiency by the photocatalytic effect while increasing the voltage. As a result, when 3 V was applied, the degradation efficiency was the best. When a voltage above that was applied, the degradation efficiency tended to be similar or rather decreased from 3 V. Therefore, the photocatalytic effect according to the flow rate was compared by applying 3 V, which has the best degradation efficiency. Comparing the photocatalytic activity of CF/TiO₂ and CF/Au/TiO₂ samples under solar simulated light, the photocatalytic degradation efficiency of R6G is improved at a slower flow rate. In addition, the surface coated with Au NPs has a better photocatalytic degradation effect than the surface coated with TiO₂ only (Fig. 5).

Conclusions

Using spray and UV irradiation-based synthesis, the Au/TiO₂ NPs were uniformly coated on the microporous layer of carbon fabric to leverage photocatalytic effects in the visible range. Comprehensive SEM, TEM, EDX, XPS, and XRD crystal structure, elemental, electrical, chemical state, interaction, and morphological analysis of the CF/Au/TiO₂ samples demonstrated and strongly supported the uniform formation of Au/TiO₂ NPs, the improvement of electron transport and charge separation, and the high photocatalytic activity of TiO₂ anatase crystal structures.

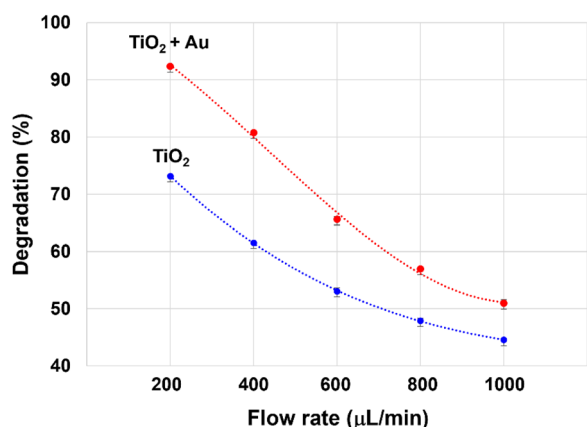


Fig. 5 A graph comparing the photocatalytic degradation of Rhodamine 6G(R6G) under the influence of applied voltage (3 V) and solar simulated light (1Sun) on CF/TiO₂ or CF/Au/TiO₂.

Using an optofluidic microreactor with a CF/Au/TiO₂ structure and solar-simulated light, higher organic degradation performance of Au/TiO₂ NPs was demonstrated as anticipated.

Acknowledgements

We thank Yunhee Lee for valuable assistance with the TEM imaging experiments, which were performed at the TEM laboratory of the center for nano materials of Sogang university. We thank Sooyeon Lee and Jihye Yu for the valuable help in the SEM imaging experiments conducted at the SEM laboratory of Sogang university.

Author contributions

ES Investigation, Methodology, Validation, Formal analysis, Writing – Original Draft, Writing – Review and Editing. JJ Methodology, Formal analysis. CW Methodology. JP Project administration, Supervision, Resources, Writing – Original Draft, Writing – Review and Editing.

Funding

This work was supported by a National Research Foundation of Korea (NRF) grant funded by the Korean government (MSIP) (2020R1A2C2009093) and by the Korea Environment Industry and Technology Institute (KEITI) through its Ecological Imitation-based Environmental Pollution Management Technology Development Project funded by the Korea Ministry of Environment (MOE) (2019002790007).

Declarations

Competing interests

The authors declare that they have no competing interests.

Received: 11 November 2023 Accepted: 7 December 2023

Published online: 15 December 2023

References

- Yuan Y-P, Ruan L-W, Barber J, Loo SCJ, Xue C (2014) Hetero-nanostructured suspended photocatalysts for solar-to-fuel conversion. *Energy Environ Sci* 7:3934–3951
- Erickson D, Sinton D, Psaltis D (2011) Optofluidics for energy applications. *Nat Photon* 5:583
- Kudo A, Miseki Y (2009) Heterogeneous photocatalyst materials for water splitting. *Chem Soc Rev* 38:253–278
- Jiang C, Moniz SJ, Wang A, Zhang T, Tang J (2017) Photoelectrochemical devices for solar water splitting—materials and challenges. *Chem Soc Rev* 46:4645–4660
- Srinivasan M, White T (2007) Degradation of methylene blue by three-dimensionally ordered macroporous titania. *Environ Sci Technol* 41:4405–4409
- Wang N, Zhang X, Wang Y, Yu W, Chan HL (2014) Microfluidic reactors for photocatalytic water purification. *Lab Chip* 14:1074–1082
- Shang J, Chai M, Zhu Y (2003) Solid-phase photocatalytic degradation of polystyrene plastic with TiO₂ as photocatalyst. *J Solid State Chem* 174:104–110
- Zhao X, Li Z, Chen Y, Shi L, Zhu Y (2007) Solid-phase photocatalytic degradation of polyethylene plastic under UV and solar light irradiation. *J Mol Catal A Chem* 268:101–106
- Wang L et al (2023) Review on optofluidic microreactors for photocatalysis. *Rev Chem Eng* 39:765–782
- Wang C, Jeon J, Seo E, Park J (2022) Ion-concentration-polarization-assisted photocatalytic reactor for highly efficient water purification. *Lab Chip* 22:2962–2970
- An T, Sun L, Li G, Gao Y, Ying G (2011) Photocatalytic degradation and detoxification of o-chloroaniline in the gas phase: mechanistic consideration and mutagenicity assessment of its decomposed gaseous intermediate mixture. *Appl Catal B* 102:140–146

12. Bianchi CL et al (2014) Photocatalytic degradation of acetone, acetaldehyde and toluene in gas-phase: comparison between nano and micro-sized TiO₂. *Appl Catal B* 146:123–130
13. Di Paola A, García-López E, Marci G, Palmisano L (2012) A survey of photocatalytic materials for environmental remediation. *J Hazard Mater* 211–212:3–29
14. Zhang R, Elzatahry AA, Al-Deyab SS, Zhao D (2012) Mesoporous titania: from synthesis to application. *Nano Today* 7:344–366
15. Shi J, Chen J, Li G, An T, Yamashita H (2017) Fabrication of Au/TiO₂ nanowires@carbon fiber paper ternary composite for visible-light photocatalytic degradation of gaseous styrene. *Catal Today* 281:621–629
16. Luttrell T et al (2014) Why is anatase a better photocatalyst than rutile? Model studies on epitaxial TiO₂ films. *Sci Rep* 4:4043

Publisher's Note

Springer Nature remains neutral with regard to jurisdictional claims in published maps and institutional affiliations.

Submit your manuscript to a SpringerOpen[®] journal and benefit from:

- ▶ Convenient online submission
- ▶ Rigorous peer review
- ▶ Open access: articles freely available online
- ▶ High visibility within the field
- ▶ Retaining the copyright to your article

Submit your next manuscript at ▶ [springeropen.com](https://www.springeropen.com)
